ELSEVIER

Polymer 41 (2000) 6285–6293

polymer

Simple shear plastic deformation behavior of polycarbonate plate II. Mechanical property characterization

C.K.-Y. Li, Z.-Y. Xia, H.-J. Sue*

Polymer Technology Center, Department of Mechanical Engineering, Texas A&M University, College Station, TX 77843-3123, USA

Received 19 August 1999; received in revised form 1 November 1999; accepted 4 November 1999

Abstract

It has been demonstrated in Part I of this research that the high degree of plastic deformation caused by the equal channel angular extrusion (ECAE) process leads to a nearly uniform molecular orientation across the extruded polycarbonate (PC) plate. In this paper, the effectiveness of the ECAE process in altering the mechanical property of PC is investigated. Significant improvements in flexural modulus and fracture toughness are observed, and are found to be closely related to the ECAE-induced molecular orientation. Microscopy observations of the fracture process show that the crack propagation direction is controlled both by the ECAE-induced molecular orientation direction and by the maximum principal stress direction, which results in the formation of hackles. Potential advantages of ECAE for fabricating polymer parts are addressed.

Keywords: Equal channel angular extrusion; Molecular orientation; Polymer strengthening

1. Introduction

It has been shown in Part I of this series that the solid-state, equal channel angular extrusion (ECAE) process is effective in shear-orienting macromolecular chains in polycarbonate (PC) plates [1]. It has also been demonstrated that ECAE can be used to tailor micrometer and/or nanometer scale anisotropy via different extrusion routes [1–5]. This paper focuses on studying how the mechanical property of PC is affected by ECAE under two different routes: route A, and route C (Fig. 1).

The uniqueness of ECAE is that it imposes a uniform, through-thickness simple shear deformation on the extrudate without altering the dimensions of extrudates. Depending on whether the polymer is a semi-crystalline polymer or an amorphous polymer, extrusion is usually performed at temperatures below the melting temperature (T_m) or the glass-transition temperature (T_g) of the polymer to slow down molecular relaxation. This leads to a significant level of molecular and/or micro-domain orientation in the polymer extrudate. The uniformity and degree of molecular orientation observed in ECAE cannot be easily achieved by any existing conventional processing means, especially when the polymer extrudate is thick (>2 mm).

The FEM modeling results obtained previously indicate that both simple shear and the high strain rate gradient across the channel intersection plane of the ECAE die (Fig. 1) are responsible for the macroscopic orientation during the ECAE process [1]. However, a thorough understanding of both mechanics and molecular orientation behavior is still needed so as to predict the molecular orientation during the ECAE process.

According to Heymans [6], all reasonably successful descriptions of the deformation behavior in polymers require the knowledge of at least two components of strain. He maintained that the Brown–Windel model [7], which divides polymer deformation into a segmental orientation part and a chain extension part, is currently the most convincing model to address molecular orientation. The necessary deformation conditions for obtaining high segmental orientation are opposite to what lead to high chain extension [8], for example, high levels of segmental orientation are achieved by rapid stretching at temperatures close to, but below T_g, which will result in low molecular chain extension. While the largest chain extension, on the other hand, is achieved at high temperatures (above T_g) by slow stretching. The discrepancy in macroscopic shear plane angle and in microscopic molecular orientation is discussed in this paper.

The main objective of this study is to investigate the effectiveness of ECAE in improving mechanical properties of PC. The relationship between the fracture process and the ECAE-induced molecular orientation is established.

* Corresponding author. Tel.: +1-409-845-5024; fax: +1-409-862-3989.
E-mail address: hjsu@acs.tamu.edu (H.-J. Sue).

0032-3861/00/$ - see front matter
PII: S0032-3861(99)00837-X

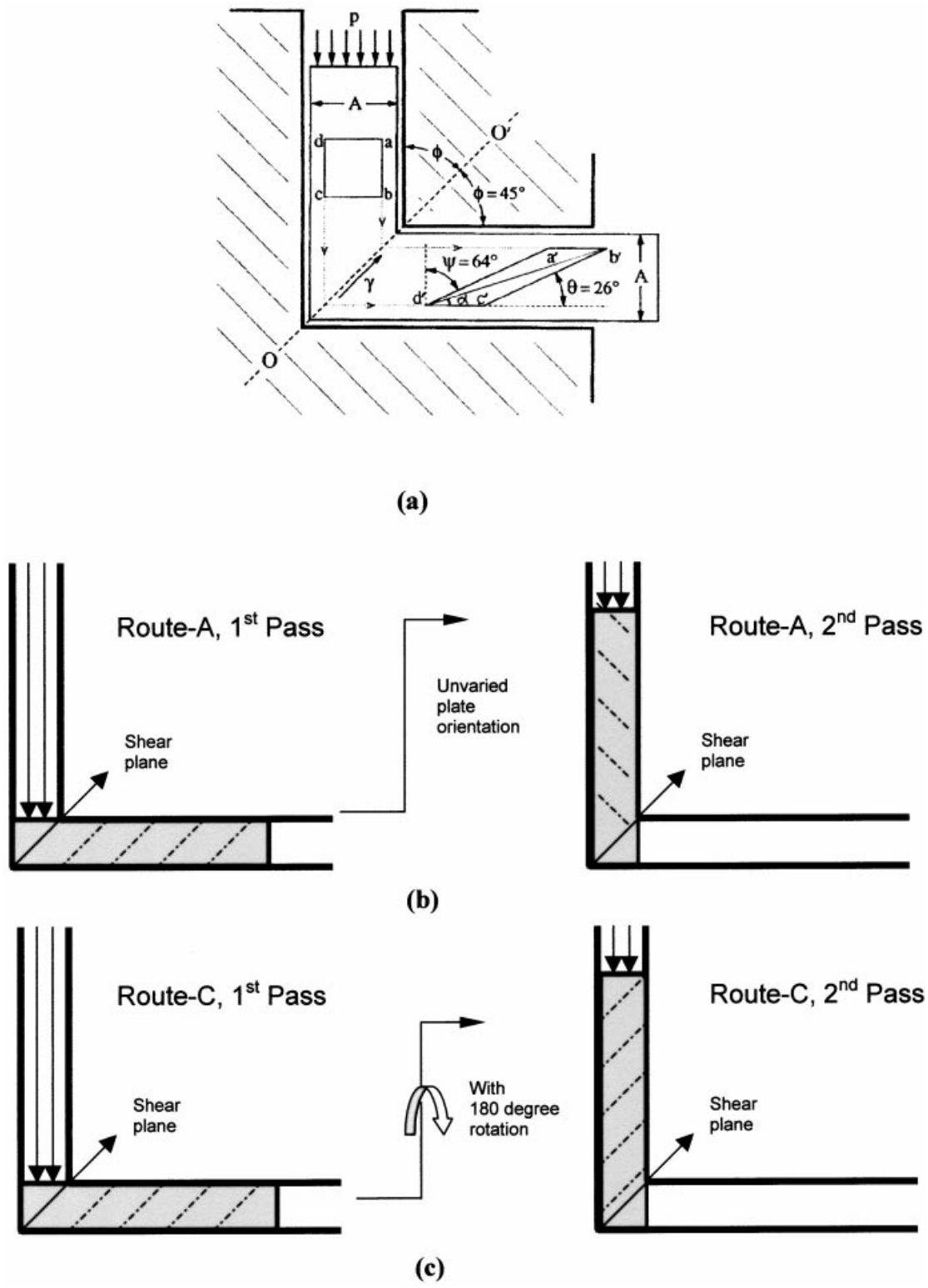

Fig. 1. (a) Schematic of polymer deformation during ECAE, showing distortion of material element (*abcd* to $a'b'c'd'$) caused by simple shear at the channel cross plane (O–O′). The shear strain, γ, caused by extrusion and occurring at the crossing plane is equal to $\tan\psi = \cot\theta = 2N\cot\phi$. The terms N and P refer to the number of extrusion passes and the extrusion pressure, respectively. (b) Schematic of route A extrusion. (c) Schematic of route C extrusion. The dash lines indicate the molecular orientation induced by the previous extrusion.

Potential significance of the ECAE process for enhancing physical and mechanical properties of polymers is also discussed.

2. Experimental

2.1. Materials and sample preparation

Extruded PC sheets (LEXAN® 103), with a density of 1.20 g/cm^3, were obtained from General Electric Company. The PC sheets are of a nominal thickness of 9.52 mm (3/8″). The sheets were machined into dimensions of $152.40 \times 152.40 \times 9.52$ mm^3(6″ × 6″ × 3/8″) to fit the die for ECAE processing. The PC plaques were then annealed for 15 h at 150°C and slowly cooled in an oven to ambient temperature to minimize the presence of pre-existing thermal history as well as residual stresses. These annealed PC plaques were carefully examined using a polariscope. Whence, few fringes were found indicating little presence of residual stresses.

2.2. The equal channel angular extrusion process

A servo-hydraulic driven mechanical testing system (MTS 810 system) was used to extrude PC plaques through the angular die set-up as shown in Fig. 1. The punch pressure and plunger traveling distance were recorded during the extrusion. An anti-seize lubricant (PERMATEX INDUSTRIAL, Type 80208) was utilized to minimize friction between the plunger and the die. The PC plaques were extruded at 100°C and at rates ranging from 0.17 to 0.51 mm/s. To experimentally measure the amount of shear strain present in the extrudate, PC plaques were milled to show square grids pattern, 1.2×1.2 mm^2 in size, throughout the thickness side of the sample surface.

In this study, the PC plaques were processed through route A, 1-pass and route C, 2-pass with the extrudate rotating by 180° about the extrusion axis on the second pass of route C [4]. The shear strain (γ) that the material experiences after one pass has been shown to be: $\gamma = \tan \Psi = \cot \theta$ (Fig. 1) [5]. For route C, 2-pass process, the material elements are deformed on the first pass and restored to their original global undeformed state on the second pass.

2.3. Dynamic mechanical analyses

Dynamic mechanical spectroscopy (DMS Rheometrics 800/RDS II) measurements were performed in a torsional mode under a fixed frequency of 1 Hz over the temperature range from −150 to 180°C. Samples were cut from the extruded plaques along the extrusion direction into dimensions of $35.5 \times 9.5 \times 3.3$ mm^3. The spectrometer was set in all cases to produce a sinusoidal peak strain amplitude of 0.05%. Measurements were made at 2.5°C intervals, and 30 s of time was allowed at each temperature setting before the final readings were taken. Temperature stability of the sample chamber is estimated to be about ±0.2°C after an initial overshoot of about 2–3°C. DMS spectra of an annealed sample and samples extruded at 1-pass and 2-pass were obtained.

2.4. Flexural modulus measurements

The flexural moduli were evaluated using a standard ASTM D-790 test method. Samples that had undergone one ECAE pass at extrusion rates of 0.17 and 0.25 mm/s were evaluated. The extruded plaques were machined into dimensions of $152 \times 13 \times 10$ mm^3 both along (longitudinal samples) and transverse (transverse samples) to the extrusion direction. They were tested in a 3-point-bend geometry using a screw-driven mechanical testing machine (Instron, Model 4411) at a constant crosshead speed of 0.07 mm/s with a supporting span length of 127 mm. Both the load and the crosshead displacement were recorded during the test. The modulus of elasticity in bending (flexural modulus) was then determined using the following equation,

$$E_B = \frac{L^3 m}{4bd^3} \quad (1)$$

where E_B is the modulus of elasticity in bending (MPa), L the support span (mm), b the width of beam tested (mm), d the thickness of beam tested (mm), and m the slope tangent to the initial straight-line portion of the load-deflection curve (N/mm).

2.5. Fracture behavior study

The fracture resistance was evaluated by measuring the plane-strain fracture toughness (the critical stress-intensity factor, K_{IC}) using a standard ASTM D-5045 test method in a single-edge-notch 3-point-bend (SEN-3PB) geometry, and by a fractographic analysis. The K_{IC} values were obtained at the self-similar region of the crack path before an impetuous change of crack propagation (Fig. 2).

SEN-3PB samples were cut from extruded plaques both parallel and perpendicular to the extrusion direction into dimensions of $89.0 \times 9.0 \times 9.4$ mm^3. These bars were then notched with a milling tool (with a tip radius of 100 μm), followed by a liquid nitrogen chilled razor blade tapping to wedge open a sharp crack. The ratio between the final crack length (a) and the specimen width (w), a/w, was held in the range between 0.3 and 0.5. A screw driven mechanical testing machine (Instron, Model 4411) was used to perform the SEN-3PB experiment. In all tests, a crosshead speed of 0.17 mm/s was applied. Both the load and the crosshead displacement were recorded during the test. The K_{IC} value was calculated from the peak load by equations that have been established on the basis of elastic stress analysis [9]. The characteristic failure patterns were investigated systematically, by observing the fractured samples using an optical

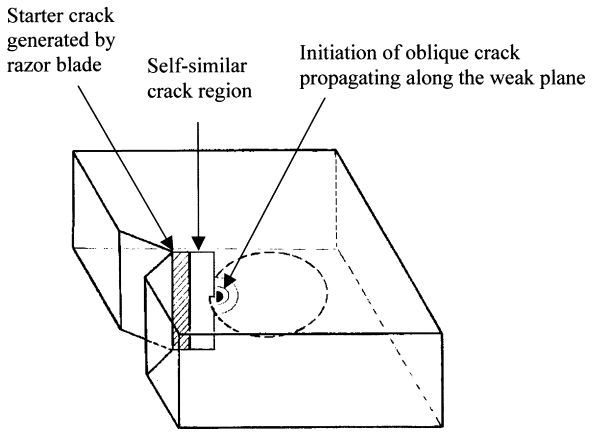

Fig. 2. An impetuous change in the crack propagation direction is observed in extruded PC samples.

microscope, Olympus BX60, under both transmitted and reflected modes.

3. Results and discussion

To study the dynamic mechanical behavior, the DMS spectra of the annealed and extruded materials are shown in Fig. 3. As expected, the extruded material is found to have higher values of G' than that of annealed material at room temperature. This indicates that higher rigidity can be achieved using ECAE. However, the onset temperatures for the T_g of the extruded materials are lower than that of the annealed sample. This implies that a change in molecular and/or segmental state packing has taken place.

The values of $\tan\delta$ for the extruded and annealed materials are essentially the same at temperatures below -60°C, but the extruded samples exhibit significantly higher $\tan\delta$ values at temperatures greater than 50°C. This finding suggests that the localized molecular-scale motions are affected little by the simple shear process, but the larger scale segmental motions at temperatures above 50°C are strongly affected by ECAE. As a result, the onset temperature for T_g is reduced due to ECAE processing. At this stage, it is still uncertain about the exact cause(s) for the change in the $\tan\delta$ curves.

The flexural modulus data, as shown in Fig. 4, indicate that the shear deformed ECAE samples exhibit a higher modulus regardless of the processing rate. Longitudinal samples show a significant increase in flexural modulus by as much as 15%. Whereas, the flexural modulus only increases slightly in the transverse sample. It is speculated that the significant increase in flexural modulus of longitudinal samples is closely related to the enhanced molecular packing along the shear plane direction. An increase in density of 0.27% after ECAE is also observed [10]. These findings indicate that the likelihood of improved molecular packing can be achieved by ECAE.

3.1. Calculation of stress-intensity factor (K) in anisotropic elastic media

The conventional fracture mechanics approach is only applicable for homogeneous, isotropic materials. It has been widely practiced in the engineering fields and found to give reasonable results.

The extrudate after the ECAE is anisotropic in nature. However, according to Sih and Williams [11,12], the general equations for crack-tip stress fields in anisotropic media can be derived by using the complex functional approach. The elastic stress singularity of the order $r^{-1/2>}$ (r being the radial distance from the crack tip) is always present at the crack tip in a medium with rectilinear anisotropy, which enables us to apply the conventional fracture mechanics approach to the fracture conditions for anisotropic media to a good approximation.

Meanwhile, Williams [12] pointed out that the K_{IC} value for a through crack in an infinite anisotropic plate loaded under a uniform pressure is exactly the same as that in the isotropic case. This finding is an important simplification for the anisotropic material. Because for a small crack in a wide plate ($a/w \ll 1$), one could still expect the isotropic result.

For a finite plate, an alternative form of K_I becomes, $K_I^2 = Y^2\sigma^2 a$, where $Y(a/w)$ is the finite width correction factor, and most of the increase in $Y^2(a/w)$ above π (for through crack in an infinite plate $K_I^2 = \pi\sigma^2 a$) is due to the increase of the net section stress resulting from the stress boundary conditions. Therefore, we would expect Y^2 not to differ greatly from the isotropic values, even for finite a/w values [12].

For arbitrary anisotropy, Gao and Chiu [13] obtained a perturbation solution in remarkably simple forms for K_I at the tip of a slightly curved finite crack under remote stresses in elastic solid. Their solution is identical to the corresponding isotropic solution derived by Cotterell and Rice [14].

The aforementioned analyses clearly indicate that under certain circumstances, the K_I in anisotropic materials can be formulated in a similar manner as in isotropic materials. Nevertheless, both approaches seem to require further modifications before a representative K_I value can be obtained for general cases. In this study, K_{IC} values were obtained in the self-similar region of the crack path (Fig. 3) using standard ASTM D-5045 testing procedures. The K_{IC} values in both the longitudinal and transverse samples were then utilized to characterize the effect of the ECAE-induced anisotropy on fracture resistance.

It is noted that the K_{IC} values measured, only represent the fracture toughness along and perpendicular to the extrusion direction. The K_{IC} values on any other directions may vary. Typical values of K_{IC} of the samples processed by route A, 1-pass and route C, 2-pass are presented in Fig. 5. For 1-pass extrusion, the longitudinal samples, in which the crack propagates perpendicular to the extrusion direction, exhibit a higher toughness by as much as 40% in K_{IC} value than that of annealed PC. On the other hand, transverse samples show

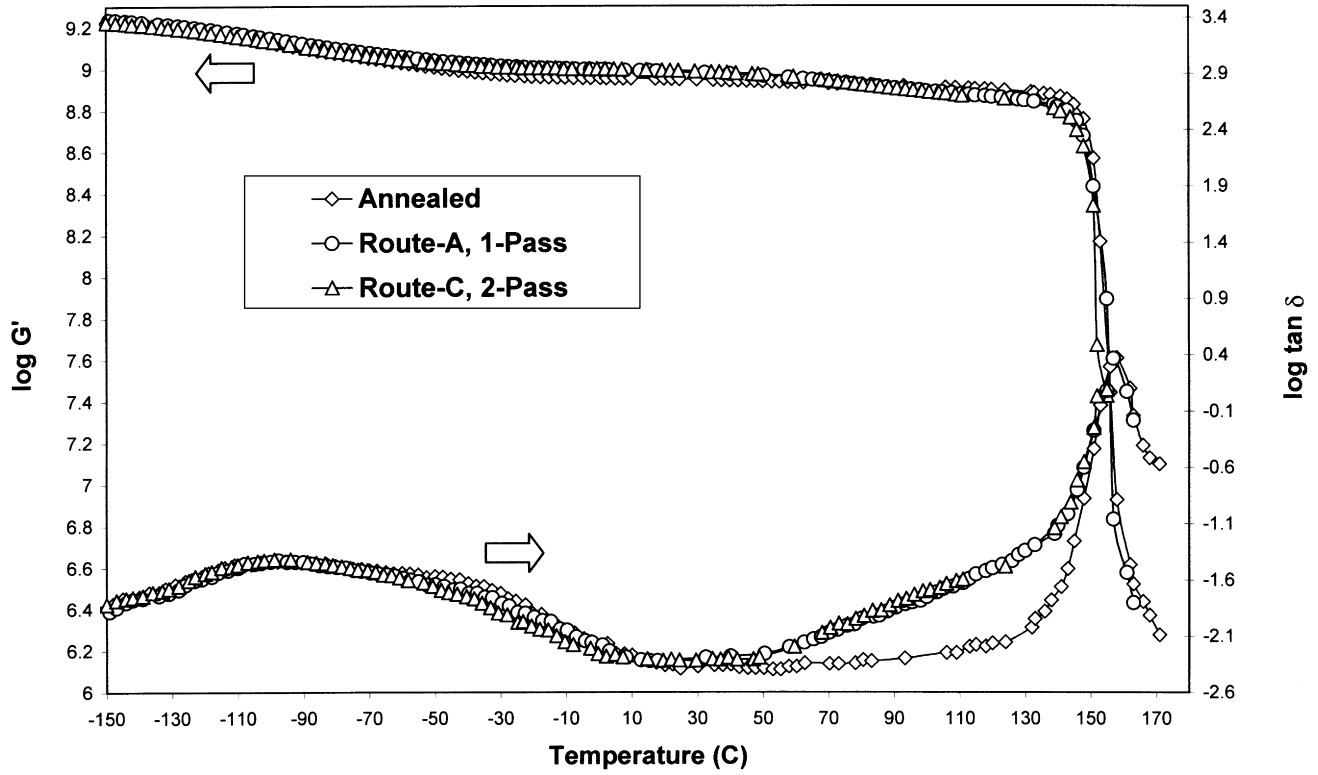

Fig. 3. Dynamic mechanical spectra of: (1) annealed PC; (2) PC after route A, 1-pass extruded at 100°C, 0.25 mm/s; (3) PC after route C, 2-pass extruded 100°C, at 0.25 mm/s.

a more limited increase in the K_{IC} values. For samples extruded by route C, 2-pass, the transverse samples are slightly tougher than the longitudinal samples. It is noted that the route C, 2-pass samples, as opposed to the route A, 1-pass samples, exhibit no weak planes. As a result, the route C, 2-pass samples are ideal for applications where material isotropy is desired.

It is recognized that molecular orientation generally

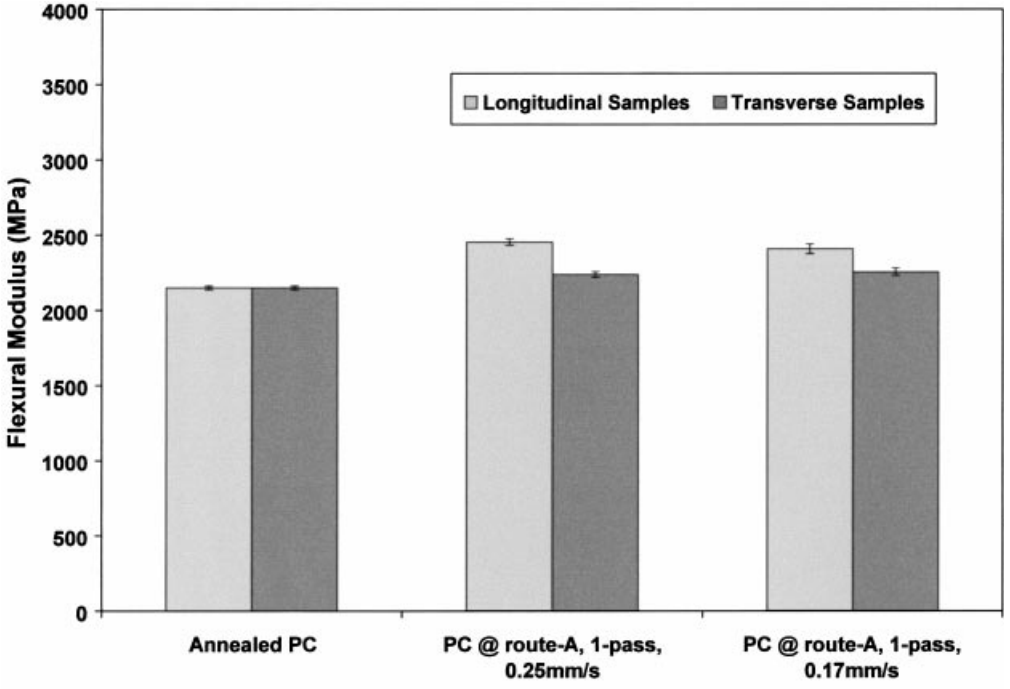

Fig. 4. Flexural modulus increases with ECAE process. PC plaques were extruded at 100°C.

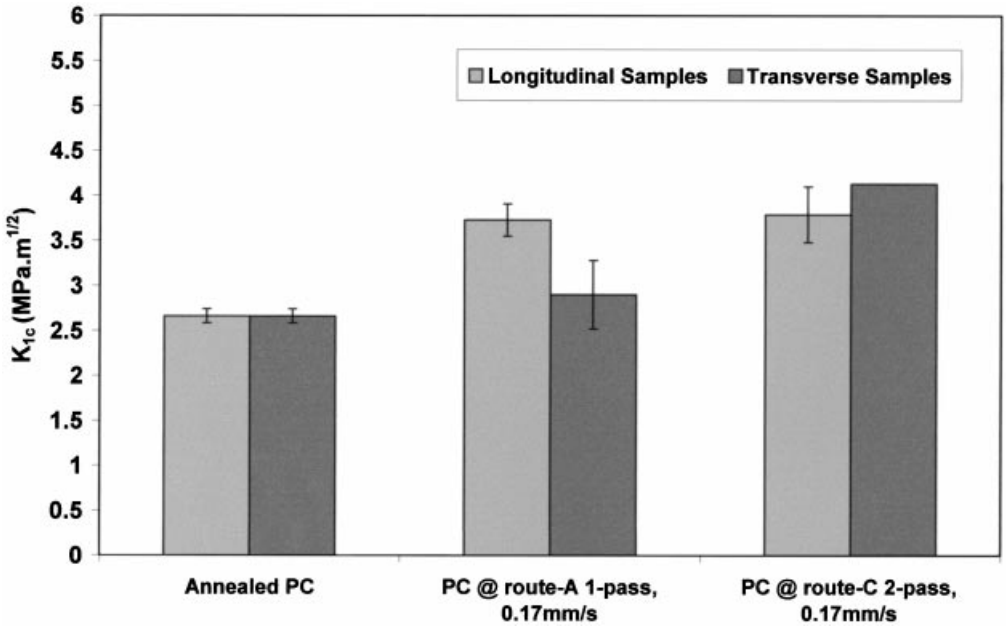

Fig. 5. The critical stress-intensity factor, K_{IC}, increases due to ECAE process. PC plates were extruded at 100°C.

enhances fracture resistance if the crack propagates at an angle to the molecular orientation direction. The fracture properties become poor if the crack propagates parallel to the orientation direction [15]. The fracture properties are affected also by the degree of orientation, the state of orientation (uniaxial vs biaxial), and by the enhanced local order of molecules. It is expected that the K_{IC} value will be the highest when the crack propagates perpendicular to the molecular orientation direction for the route A, 1-pass sample.

As shown in Fig. 6, the annealed PC exhibit a brittle fracture behavior regardless of the crack propagation direction. This implies that a nearly isotropic state is obtained after annealing. When the load is applied, the sharp crack propagates straight-ahead, leaving few features on the fracture surfaces. This indicates that the fracture surfaces contain topographic irregularities smaller than the wavelength of light. Contrary to this, once molecular orientation is introduced into the sample, complex fracture features are observed due to the impetuous alteration of the crack path (Figs. 7 and 8).

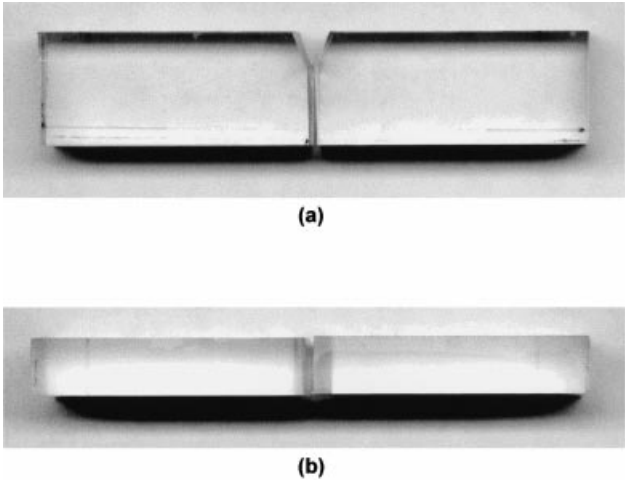

Fig. 6. Annealed 3-point-bend test specimens of PC: (a) top view; (b) side view.

We have demonstrated in Part I of this research [1] that in the 1-pass samples, the average molecular orientation angle, α, is at about 28° counterclockwise away from the extrusion direction. The most probable molecular orientation should be along the maximum shear strain direction, i.e. the principal axis of the strain ellipse as has been shown in Ref. [10]. So, there is a discrepancy between the macroscopic shear plane angle, θ and the microscopic molecular orientation angle, α, as can be seen in Fig. 1a. These two angles are related by the following formulae:

$$\gamma = \cot\theta \tag{2}$$

$$\alpha = \frac{1}{2}\tan^{-1}\left(\frac{2}{\gamma}\right) \tag{3}$$

$$\tan(2\alpha) = 2\tan\theta \tag{4}$$

Based on Eq. (4), α equals θ when they are small. The macroscopic shear plane angle, θ, is found to be closely related to the strain hardening characteristics of PC [10].

A crack is most likely to propagate along the molecular orientation plane, i.e. along the weak plane. Figs. 7b and 8b clearly show that the inclined crack planes with respect to the extrusion direction are indeed nearly coincident with the molecular orientation plane. Likewise, a distinctive crack pattern is observed due to biaxial molecular orientation in

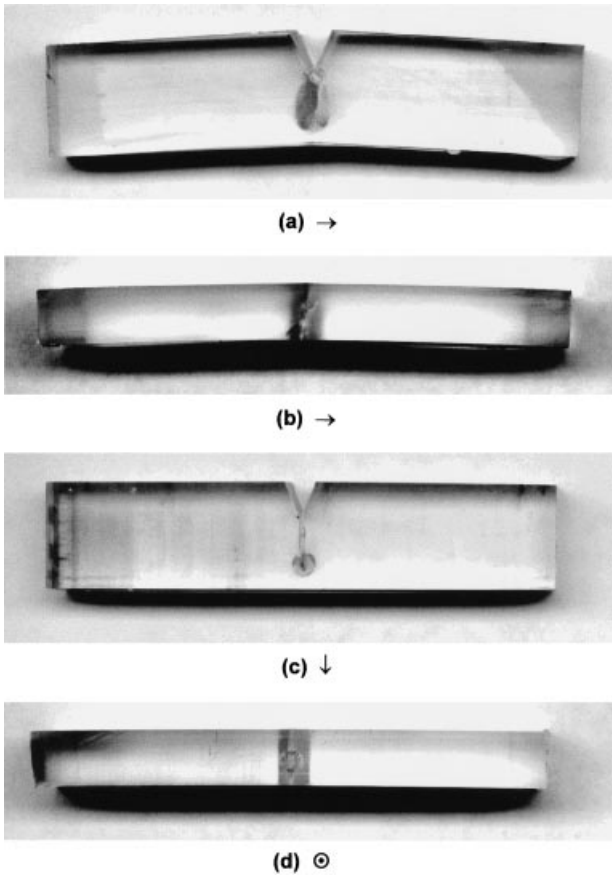

Fig. 7. The 3-point-bend test specimens of PC processed under route A, 1-pass extruded at 0.17 mm/s at 100°C: (a) longitudinal sample, top view; (b) side view; (c) transverse sample, top view; (d) side view. Arrows indicate the extrusion direction.

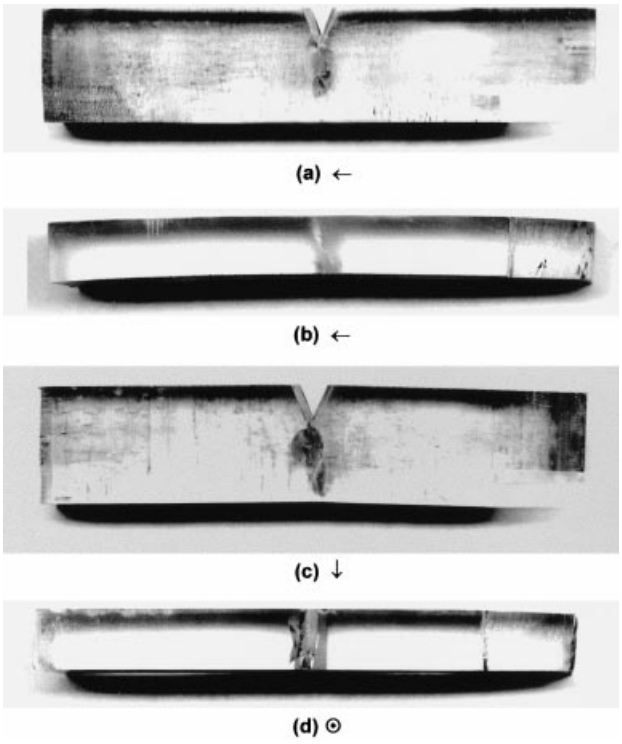

Fig. 8. The 3-point-bend test specimens of PC processed under route C, 2-pass extruded at 0.17 mm/s at 100°C: (a) longitudinal sample, top view; (b) side view; (c) transverse sample, top view; (d) side view. Arrows indicate the extrusion direction of the second pass.

the route C, 2-pass samples (Figs. 8a, c and d). A detailed investigation in crack propagation is thus required to correlate the extrusion routes with the induced molecular orientation.

Figs. 9 and 10 show that samples extruded through the same route exhibit similar fracture characteristics regardless of the extrusion rates used in this study. A common feature of the longitudinal samples is that the initial sharp crack grows in a slanted manner. Intuitively, the crack front seeks a weak plane along which to propagate rather than breaking the aligned macromolecular chains. As a result, hackles are formed (Fig. 11). Secondary cracks are also observed around the crack tip, thus complicating the fractographic features. For the transverse samples, the crack seems to propagate rectilinearly leaving fewer features in its wake.

One of the unique features in the samples that underwent route C, 2-pass extrusion is the localized orientation state. As indicated in Fig. 8b, the second pass seems to introduce an opposite local molecular orientation in addition to cancelling out the previous global deformation due to the first pass extrusion. In other words, each pass in the 2-pass ECAE is effective in aligning molecules along one distinctive shear plane. This results in a molecularly biaxial-state orientation (Fig. 10b and d). Therefore, the macroscopic scale of orientation is restored while the localized molecular conformation remains highly oriented.

The localized oriented state caused by route C, 2-pass extrusion is also effective in generating hackles (Fig. 11b). This is similar to what occurs in the 1-pass samples (Fig. 11a). Contrary to the 1-pass samples, the presence of a macroscopic weak plane is not observed in the 2-pass samples. This, in turn, leads to an improved fracture resistance in all directions (Fig. 5).

The significance of ECAE lies in that it provides means to precisely control the degree and direction of micro-domain and/or molecular orientation even in bulky polymer extrudates. This can be achieved by implementing ECAE through cumulative extrusions and distinct extrusion routes. Moreover, the dimensions of the extrudate remain constant during the fabrication process. It is expected that the ECAE process is particularly useful for load-bearing substructures where rigidity and fracture resistance are of primary concerns.

Thus far, we have demonstrated that well-controlled morphology can lead to great improvements in mechanical properties. The implementation of ECAE can therefore make the polymer extrudates tougher without the need of toughenes, such as rubbers and short fibers. The polymer extrudates can also exhibit improved rigidity,

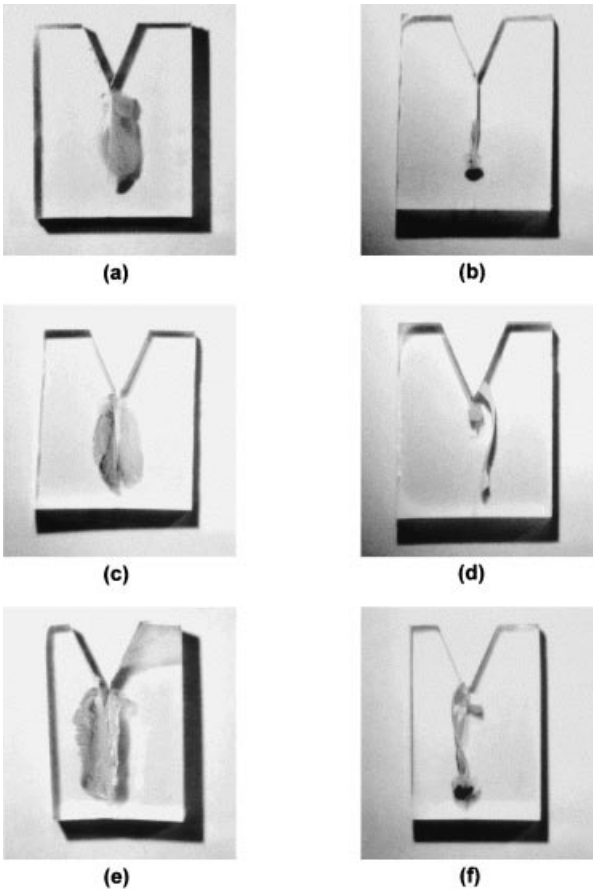

Fig. 9. Detailed crack propagation characteristics of 1-pass samples: (a) longitudinal sample at an extrusion rate of 0.51 mm/s; (b) transverse sample at 0.51 mm/s; (c) longitudinal sample at 0.25 mm/s; (d) transverse sample at 0.25 mm/s; (e) longitudinal sample at 0.17 mm/s; (f) transverse sample at 0.17 mm/s.

strength, barrier properties, and, most likely, impact resistance [16]. ECAE can be extended to orient molecules and dispersing second-phase domains in polymer blends and filled polymers. Optimized morphology and property in polymeric systems can be realized if the ECAE concept can be successfully implemented in polymer processing.

4. Conclusion

The effectiveness of the ECAE process in controlling polymer molecular anisotropy is investigated. The experimental results suggest that the large strain plastic deformation induced by ECAE, not only generates a high degree of molecular orientation but also gives better molecular packing. The mechanical properties can be tailored by extruding the material via various processing scenarios, i.e. by changing extrusion routes and the number of extrusion passes. Significant impact is expected in utilizing ECAE to fabricate engineering polymer components.

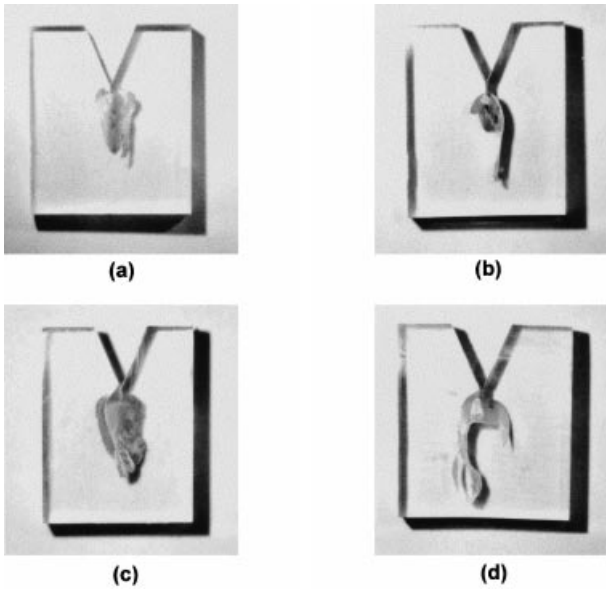

Fig. 10. Detailed crack propagation characteristics of 2-pass, route C samples: (a) longitudinal sample extruded at 0.25 mm/s; (b) transverse sample at 0.25 mm/s; (c) longitudinal sample at 0.17 mm/s; (d) transverse sample at 0.17 mm/s.

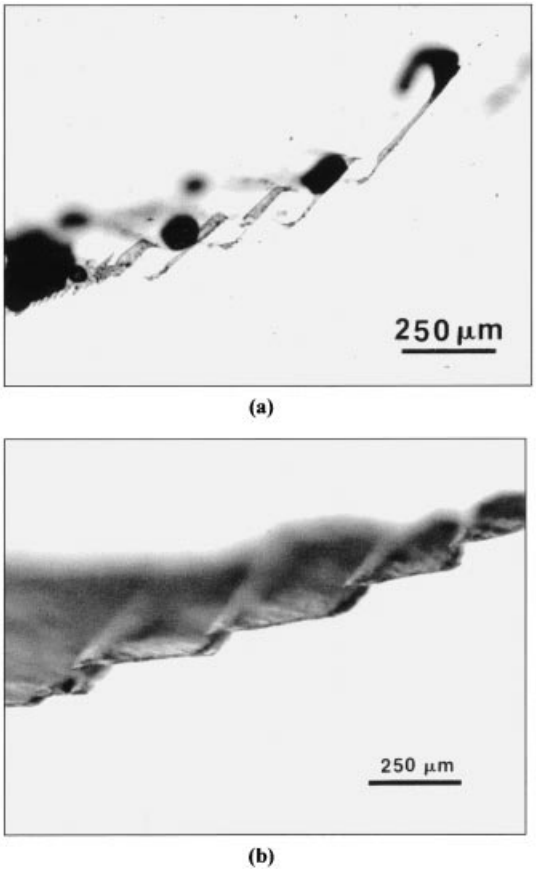

Fig. 11. (a) Hackles are observed at the crack tip of 1-pass PC sample; (b) Hackles are observed in route C, 2-pass PC sample, similar to that observed in the 1-pass samples.

Acknowledgements

The authors would like to thank Drs K. Ted. Hartwig Jr., R. E. Goforth, H.-J. Cui, and R.E. Barber for their insightful discussion and experimental assistance with this work. Research grants from Dow Chemical and the State of Texas (Grant #APR-98-32191-72380) are greatly appreciated.

References

[1] Sue H-J, Dilan H, Li K-Y. Polym Engng Sci 1999; in press.
[2] Dilan H. MS thesis, Texas A&M University, College Station, 1996.
[3] Sue H-J, Li K-Y. J Mater Sci Lett 1998;17:853.
[4] Segal VM, Hartwig KT, Goforth RE. Mater Sci Engng A 1997;224:107.
[5] Ferrasse S, Segal VM, Hartwig KT, Goforth RE. Metall Mater Trans A 1997;28:1047.
[6] Heymans N. Polymer 1987;28:2009.
[7] Brown DJ, Windel AH. J Mater Sci 1984;19:1997.
[8] Lundberg L, Stenberg B, Jansson J-F. Macromolecules 1996;29:6256.
[9] Anderson TL. Fracture mechanics: fundamentals and applications. 2. Boca Raton, FL: CRC Press, 1995.
[10] Li Chris K-Y. PhD dissertation, Texas A&M University, College Station, 1999.
[11] Sih GC, Paris PC, Irwin GR. Int J Frac Mech 1965;1:189.
[12] Williams JG. In: Friedrich K, editor. Application of fracture mechanics to composite materials, Amsterdam: Elsevier, 1989 chap. 1.
[13] Gao H, Chiu C. Int J Solid Struct 1992;29(8):947.
[14] Cotterell B, Rice JR. Int J Frac 1980;16:155–69.
[15] Nielsen LE, Landel RF. Mechanical properties of polymers and composites. 2. New York: Marcel Dekker, 1994.
[16] Xia Z-Y, Sue H-J, Hsieh A. In preparation.